6

Using Soil Moisture Data to Estimate Evapotranspiration and Development of a Physically Based Root Water Uptake Model

Nirjhar Shah[1], Mark Ross[2] and Ken Trout[2]
[1]*AMEC Inc. Lakeland, FL*
[2]*Univ. of South Florida, Tampa, FL*
USA

1. Introduction

In humid regions such as west-central Florida, evapotranspiration (ET) is estimated to be 70% of precipitation on an average annual basis (Bidlake et al. 1993; Knowles 1996; Sumner 2001). ET is traditionally inferred from values of potential ET (PET) or reference ET (Doorenabos and Pruitt 1977). PET data are more readily available and can be computed from either pan evaporation or from energy budget methods (Penman 1948; Thornthwaite 1948; Monteith 1965; Priestly and Taylor 1972, etc.). The above methodology though simple, suffer from the fact that meteorological data collected in the field for PET are mostly under non-potential conditions, rendering ET estimates as erroneous (Brutsaert 1982; Sumner 2006). Lysimeters can be used to determine ET from mass balance, however, for shallow water table environments, they are found to give erroneous readings due to air entrapment (Fayer and Hillel 1986), as well as fluctuating water table (Yang et al. 2000). Remote sensing techniques such as, satellite-derived feedback model and Surface Energy Balance Algorithm (SEBAL) as reviewed by Kite and Droogers (2000) and remotely sensed Normalized Difference Vegetation Index (NDVI) as used by Mo et al. (2004) are especially useful for large scale studies. However, in the case of highly heterogeneous landscapes , the resolution of ET may become problematic owing to the coarse resolution of the data (Nachabe et al. 2005). The energy budget or eddy correlation methodologies are also limited to computing net ET and cannot resolve ET contribution from different sources. For shallow water table environments, continuous soil moisture measurements and water table estimation have been found to accurately determine ET (Nachabe et al. 2005; Fares and Alva 2000). Past studies, e.g., Robock et al. (2000), Mahmood and Hubbard (2003), and Nachabe et al. (2005), have clearly shown that soil moisture monitoring can be successfully used to determine ET from a hydrologic balance. The approach used herein involves use of soil moisture and water table data measurements. Using point measurement of soil moisture and water table observations from an individual monitoring well ET values can be accurately determined. Additionally, if similar measurements of soil moisture content and water table are available from a set of wells along a flow transect , other components of water budgets and attempts to comprehensively resolve other components of the water budget at the study site.
The following section describes a particular configuration of the instruments, development of a methodology, and an example case study where the authors have successfully applied

measurement of soil moisture and water table in the past to estimate and model ET at the study site. The authors also used the soil moisture dataset to compute actual root water uptake for two different land-covers (grassed and forested). The new methodology of estimating ET is based on an eco-hydrological framework that includes plant physiological characteristics. The new methodology is shown to provide a much better representation of the ET process with varying antecedent conditions for a given land-cover as compared to traditional hydrological models.

2. Study site

The study site for gathering field data and using it for ET estimation and vadose zone process modeling was located in the sub basin of Long Flat Creek, a tributary of the Alafia River, adjacent to the Tampa bay regional reservoir, in Lithia, Florida. **Figure 1** shows the regional and aerial view of the site location. Two sets of monitoring well transects were installed on the west side of Long Flat Creek. One set of wells designated as PS-39, PS-40, PS-41, PS-42, and PS-43 ran from east to west while the other set consisting of two wells was roughly parallel to the stream (Long Flat Creek), running in the North South direction. The wells were designated as USF-1 and USF-3.

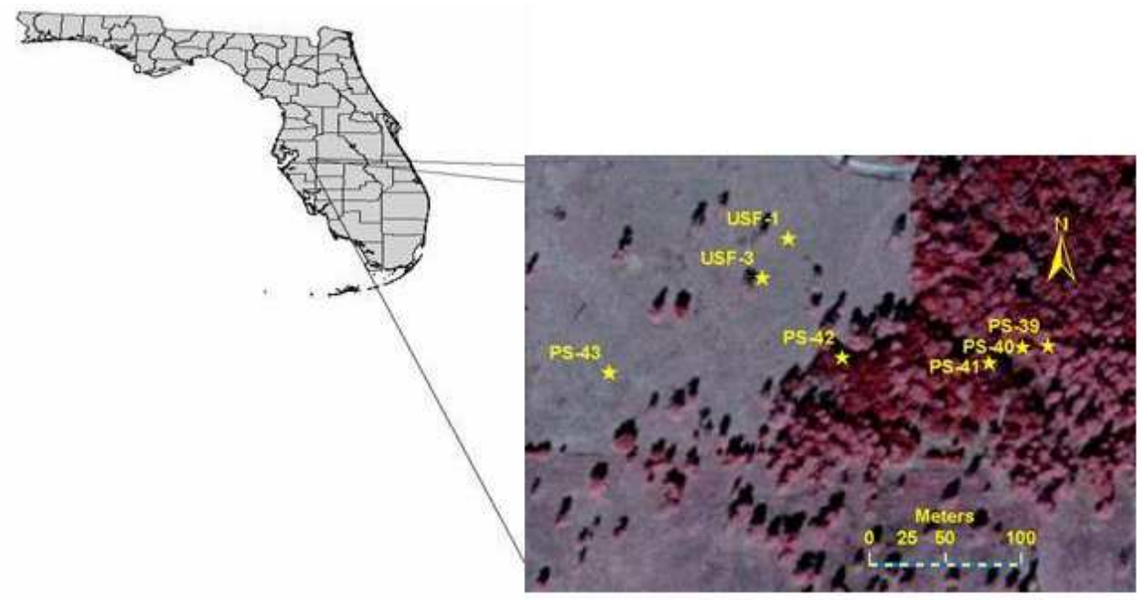

Fig. 1. Location of the study site in Hillsborough County, Florida

The topography of the area slopes towards the stream with PS-43 being located at roughly the highest point for both transects. The vegetation varied from un-grazed Bahia pasture grass in the upland areas (in proximity of PS-43, USF-1, and USF-3), to alluvial wetland forest comprised of slash pine and hardwood trees near the stream. The area close to PS-42 is characterized as a mixed (grassed and forested) zone. Horizontal distance between the wells is approximately 16, 22, 96, 153 m from PS-39 to PS-43, with PS-39 being approximately 6 m from the creek. The horizontal distance between USF-1 and USF-3 was 33 m. All wells were surveyed and land surface elevations were determined with respect to National Geodetic Vertical Datum 1929 (NGVD).

The data captured from this configuration was used both for point estimation as well as transect modeling, however , for this particular chapter, only point estimation of ET and and point data set will be used to develop conceptualizations of vadose zone processes will be discussed. For details regarding transect modeling to generate water budget estimates refer to Shah (2007).

3. Instrumentation

For measurement of water table at a particular location a monitoring well instrumented with submersible pressure transducer (manufactured by Instrumentation Northwest, Kirkland, WA) 0-34 kPa (0-5 psi), accurate to 0.034 kPa (0.005 psi) was installed. Adjacent to each well, an EnviroSMART® soil moisture probe (Sentek Pty. Ltd., Adelaide, Australia) carrying eight sensors was installed (see **Figure 2**). The soil moisture sensors allowed measurement of volumetric moisture content along a vertical profile at different depths from land surface. The sensors were deployed at 10, 20, 30, 50, 70, 90, 110, 150 cm from the land surface. The sensors work on the principle of frequency domain reflectometery (FDR) to convert electrical capacitance shift to volumetric water content ranging from oven dryness to saturation with a resolution of 0.1% (Buss 1993). Default factory calibration equations were used for calibrating these sensors. Fares and Alva (2000) and Morgan et al. (1999) found no significant difference in the values of observed recorded water content from the sensors when compared with the manually measured values. Two tipping bucket and two manual rain gages were also installed to record the amount of precipitation.

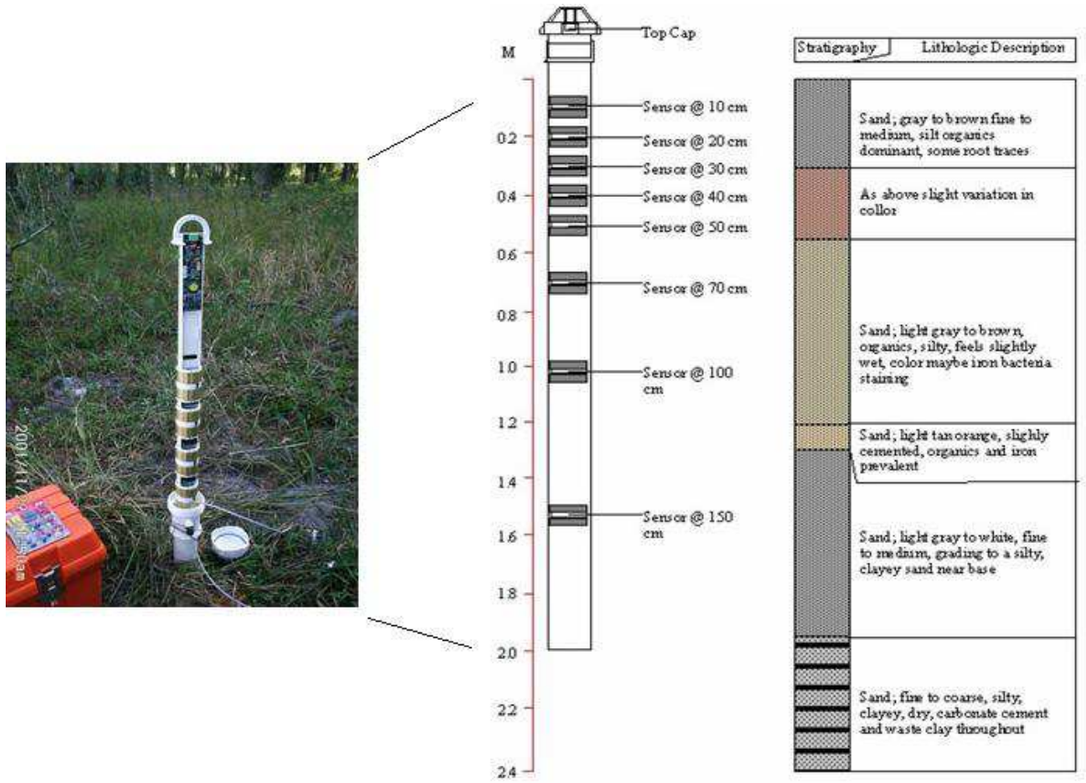

Fig. 2. Soil moisture probe on the left showing the mounted sensors along with schematics on the right showing sample stratiagraphy at different depths.

4. Point estimation of evapotranspiration using soil moisture data

At any given well location variation in total soil moisture on non-rainy days can be due to (a) subsurface flow from or to the one dimensional soil column (0 – 155 cm below land surface) over which soil moisture is measured, and (b) evapotranspiration from this soil column. Mathematically

$$\frac{\partial TSM}{\partial t} = Q - ET \tag{1}$$

where t is time [T], Q is subsurface flow rate [LT^{-1}], and ET is evapotranspiration rate [LT^{-1}]. TSM is total soil moisture, determined as below

$$TSM = \int_{\varsigma} \theta \, dz \tag{2}$$

where θ[L^3L^{-3}] is the measured water content, z [L] is the depth below land surface ς[L] is the depth of monitored soil column (155 cm). The values in the square brackets (for all the variables) represent the dimensions (instead of units) e.g. L is length, T is time.

The negative sign in front of ET in **Equation 1** indicates that ET depletes the TSM in the column. The subsurface flow rate can be either positive or negative. In a groundwater discharge area, the subsurface flow rate, Q, is positive because it acts to replenish the TSM in the soil column (Freeze and Cherry, 1979). Thus, this flow rate is negative in a groundwater recharge area. **Figure 3** illustrates the role of subsurface flow in replenishing or depleting total soil moisture in the column. An inherent assumption in this approach is that the deepest sensor is below the water table which allows accounting for all the soil moisture in the vadose zone. Hence, monitoring of water table is critical to make sure that the water table is shallower than the bottom most sensor. To estimate both ET and Q in **Equation 1**, it was important to decouple these fluxes. In this model the subsurface flow rate was estimated from the diurnal fluctuation in TSM. Assuming ET is effectively zero between midnight and 0400 h, Q can be easily calculated from **Equation 3** using:

$$Q = \frac{TSM_{0400h} - TSM_{midnight}}{4} \tag{3}$$

where TSM_{0400h} and $TSM_{midnight}$ are total soil moisture measured at 0400 h and midnight, respectively. The denominator in **Equation 3** is 4 h, corresponding to the time difference between the two TSM measurements. The assumption of negligible ET between midnight and 0400h is not new, but was adopted in the early works of White (1932) and Meyboom (1967) in analyzing diurnal water table fluctuation. It is a reasonable assumption to make at night when sunlight is absent.

Taking Q as constant for a 24h period (White 1932; Meyboom, 1967), the ET consumption in any single day was calculated from the following equation

$$ET = TSM_j - TSM_{j+1} + 24 \times Q \tag{4}$$

where TSM_j is the total soil moisture at midnight on day j, and TSM_{j+1} is the total soil moisture 24h later (midnight the following day). Q is multiplied by 24 as the **Equation 4**

provides daily ET values. **Figure 4** show a sample observations for 5 day period showing the evolution of TSM in a groundwater discharge and recharge area respectively. Also marked on the graphs are different quantities calculated to determine *ET* from the observations.

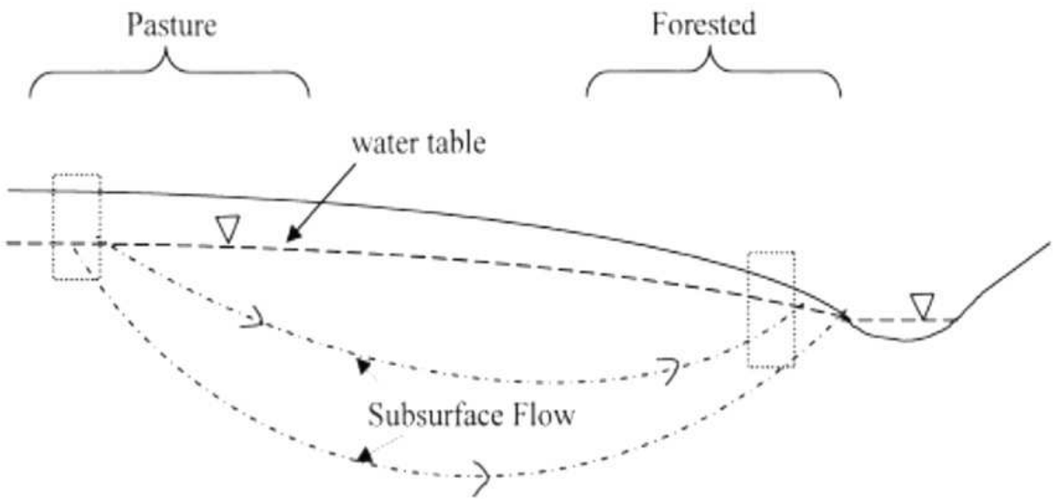

Fig. 3. Total soil moisture is estimated in two soil columns. The first is in a groundwater recharge area (pasture), and the second is in a groundwater discharge area (forested). In a groundwater discharge area, subsurface flow acts to replenish the total soil.

Equation 1 applies for dry periods only, because it does not account for the contribution of interception storage to ET on rainy days. Also, the changes in soil moisture on rainy days can occur due to other processes like infiltration, upstream runoff infiltration (as will be discussed later) etc. The results obtained from the above model were averaged based on the land cover of each well and are presented as ET values for grass or forested land cover. The values for the grassed land cover were also compared against ET values derived from pan evaporation measurements.

The ET estimates from the data collected at the study site using the above methodology are shown in **Figure 5**. **Figure 5** shows variability in the values of *ET* for a period of about a year and half. It can be seen from **Figure 5** that the method was successful in capturing spatial variability in the ET rates based on the changes in the land cover, as the ET rate of forested (alluvial wetland forest) land cover was found to be always higher than that of the grassland (in this case un-grazed Bahia grass). In addition to spatial variability, the method seemed to capture well the temporal variability in ET. The temporal variability for this particular analysis existed at two time scales, a short-term daily variation associated with daily changes in atmospheric conditions (e.g. local cloud cover, wind speed etc.) and a long-term, seasonal, climatic variation. The short-term variation tends to be less systematic and is demonstrated in **Figure 5** by the range marks. The seasonal variation is more systematic and pronounced and is clearly captured by the method.

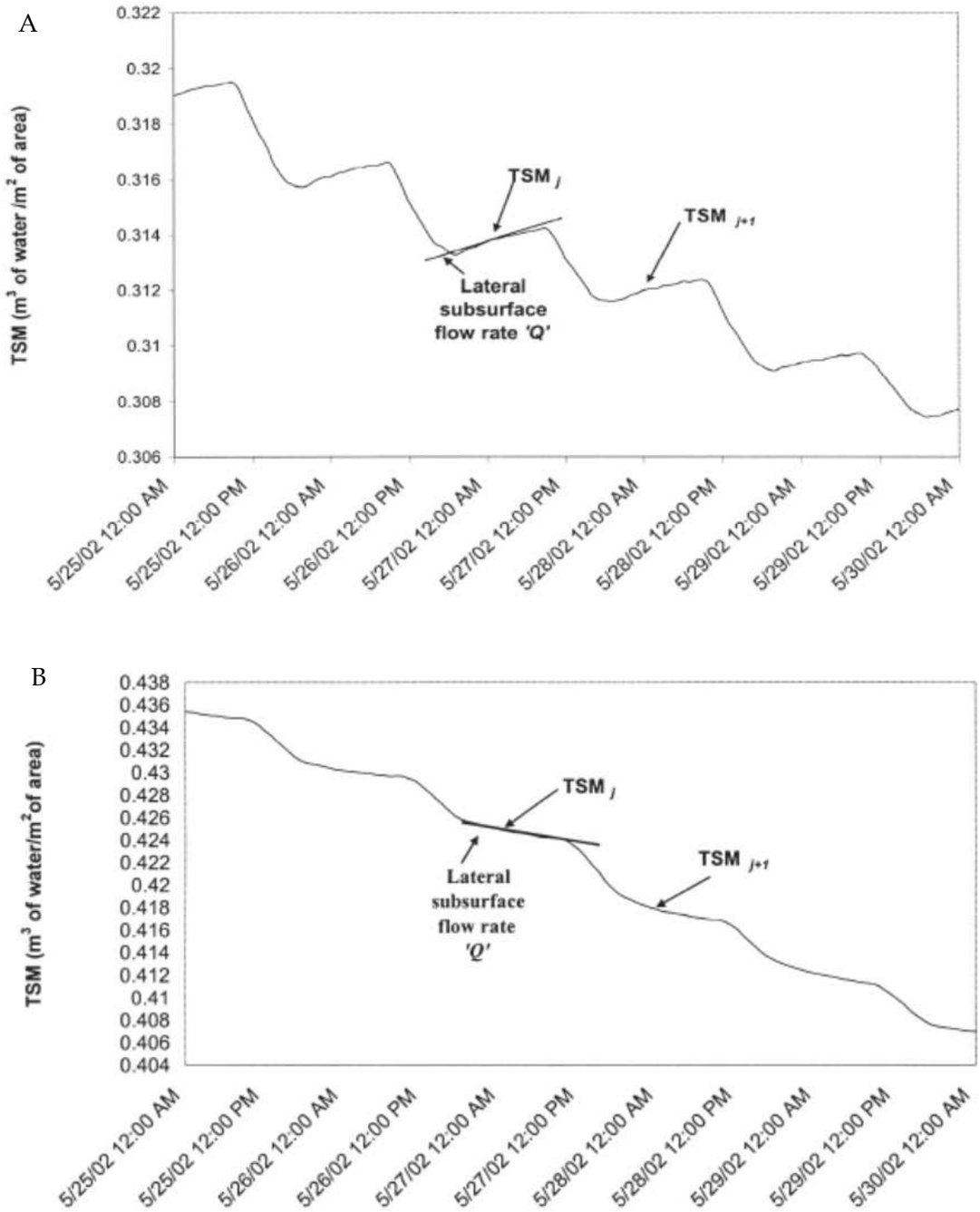

Fig. 4. Total soil moisture versus time in the (a) groundwater discharge area and (b) ground water recharge area. The subsurface flux is the positive slope of the line between midnight and 4 AM.

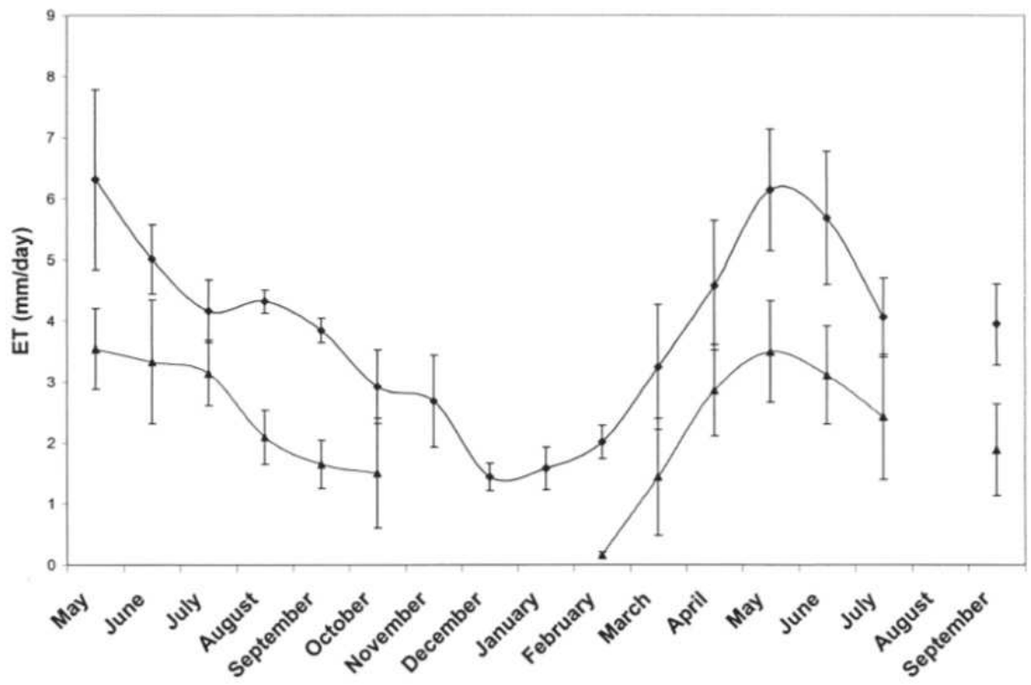

Fig. 5. Monthly average of evapotranspiration (ET) daily values in forested (diamonds) and pasture (triangles) areas. The gap in the graph represents a period of missing data. Standard deviations of daily values are also shown in the range limits.

To assess the reasonableness of the methodology, the estimated ET values for pasture were compared with ET estimated from the evaporation pan. The measured pan evaporation was multiplied by a pan coefficient for pasture to estimate ET for this vegetation cover. A monthly variable crop coefficient was adopted (Doorenbos and Pruitt, 1977) to account for changes associated with seasonal plant phenology (see **Table 1**). The consumptive water use or the crop evapotranspiration is calculated as:

$$ET_C = E_P \times K_C \tag{5}$$

where E_P is the measured pan evaporation, K_C is a pan coefficient for pastureland, and ET_C is the estimated evapotranspiration [LT^{-1}] (mm/d) by the pan evaporation method. **Figure 6** compares the ET estimated by both the evaporation pan and moisture sensors for pasture. Although the two methods are fundamentally different, on average, estimated *ET* agreed well with an R^2 coefficient of 0.78. This supported the validity of the soil moisture methodology, which further captured the daily variability of ET ranging from a low of 0.3 mm/d to a maximum of 4.9 mm/d. The differences between the two methods can be attributed to fundamental discrepancies. The pan results are based on atmospheric potential with crude average monthly coefficients while the TSM approach inherently incorporates plant physiology and actual moisture limitations. Indeed, both methods suffer from limitations. The pan coefficient is generic and does not account for regional variation in vegetation phenology or other local influences such as soil texture and fertility. Similarly, the accuracy of the soil moisture method proposed in this study depends on the number of sensors used in monitoring total moisture in the soil column.

Month		Coefficient
January		0.4
February		0.45
March		0.55
April		0.64
May		0.7
June		0.7
July		0.7
August		0.7
September		0.7
October		0.6
November		0.5
December		0.5

Table 1. Pan coefficients used to obtain pasture evapotranspiration for different months.

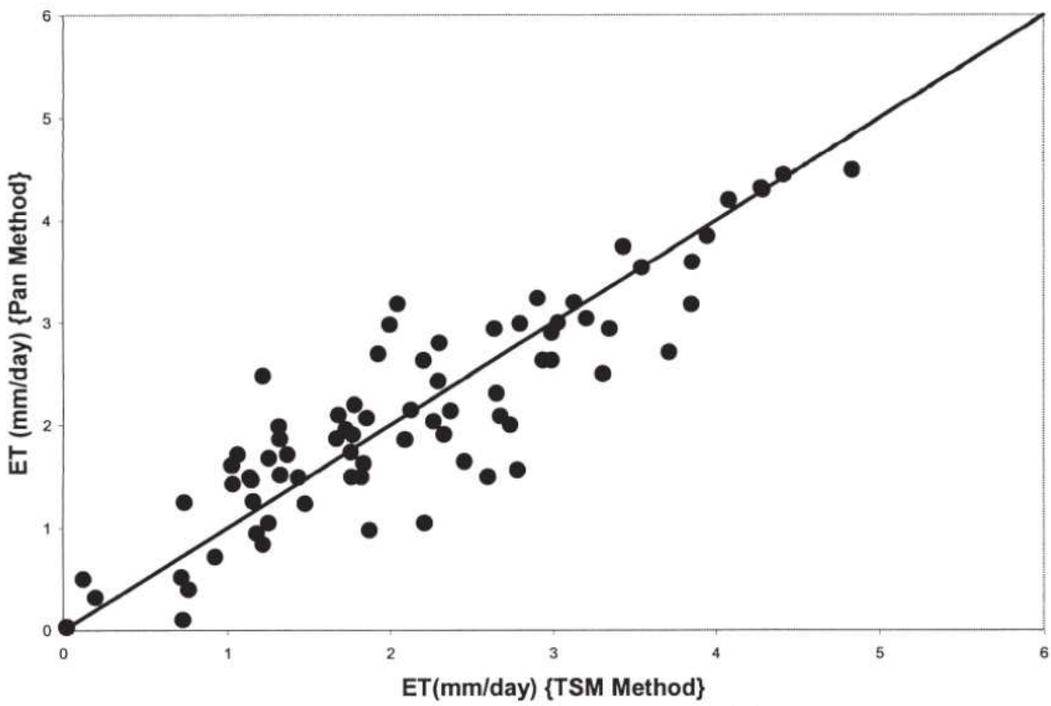

Fig. 6. Evapotranspiration estimates for pasture by the pan and point scale model. Data points represent the daily values of ET from both techniques.

5. Development of root water uptake model

The preceding sections described a novel data collection approach that can be used to measure ET (and other water budget components). The measured values can be subsequently used to develop modeling parameters or validate modeling results for areas which are similar to the study site in terms of climatic and land-cover conditions. The next step is the development of a generic modeling framework to accurately determine ET.

Transpiration by its very nature is a process that is primarily based on plant physiology and the better one can determine root water uptake the more accurate will be the estimation of actual transpiration and, therefore ET. Traditionally used models and concepts, however, make over simplifying assumptions about plants (Shah et al. 2007), hence casting doubt on the model results. What needs to be done is to try and combine land cover characteristics in the root water uptake models to produce more reliable results. With this intent in mind, recently, a new branch of study called "Eco-Hydrology" has been initiated. The aim of eco-hydrology is to encourage the interdisciplinary work on ecology and hydrology with an objective of improving hydrological modeling capabilities.
Soil moisture datasets (as described in Section 2) can be used to provide insight into the process of root water uptake which can then be combined with plant characteristics to develop a more physically based ET model. The next sections describe how the soil moisture dataset has been used by the authors to estimate vertical distribution of root-water uptake for two land-cover classes (shallow rooted and deep rooted) and how the results were then used to develop a land-cover based modeling framework.

5.1 Traditional root water uptake models

The governing equation for soil moisture dynamics in the unsaturated soil zone is the Richards's equation (Richards 1931). Richards's equation is derived from Darcy's law and the continuity equation. What follows is a brief description of Richards's equation and how can it incorporates root water uptake. For more detailed information about formulation of Richards's equation, including its derivation in three dimensions, the readers are directed to any text book on soil physics e.g. Hillel (1998).
Due to ease of measurement and conceptualization, energy of water (E) is represented in terms of height of liquid column and is called the hydraulic head (h). It is defined as the total energy of water per unit weight. Mathematically hydraulic head, h, can be represented as

$$h = \frac{E}{\rho_W g} \tag{6}$$

where ρ_W is the density of water and g is the acceleration due to gravity. The flow of water always occurs along decreasing head. In soil physics the fundamental equation used to model the flow of water along a head gradient is known as Darcy Law (Hillel 1998). Mathematically the equation can be written as

$$q = K\frac{\Delta h}{l} \tag{7}$$

where q [$L^3L^{-2}T^{-1}$] is known as the specific discharge and is defined as the flow per unit cross-sectional area, K[LT^{-1}] is termed as the hydraulic conductivity, which indicates ease of flow, Δh [L] is the head difference between the points of interest and l[L] is the distance between them. Darcy's Law is analogous to Ohm's law with head gradient being analogous to the potential difference and current being analogous to specific discharge and hydraulic conductivity being similar to the conductance of a wire.
The second component of Richards's equation is the continuity equation. Continuity equation is based on the law of mass conservation, and for any given volume it states that

net increase in storage in the given volume is inflow minus sum of outflow and any sink present in the volume of soil. Mathematically, it is this sink term that allows the modeling of water extracted from the given volume of soil.

In one dimension for flow occurring in the vertical direction (z axis is positive downwards) Richards's equation can be written as

$$\left(\frac{\partial\theta}{\partial t}\right)=\left(\frac{\partial}{\partial z}K\left(\frac{\partial h}{\partial z}+1\right)\right)-S \tag{8}$$

where θ is the water content, defined as the ratio of volume of water present and total volume of the soil element , t is time, S represents the sink term while other terms are as defined before.

If flow in X and Y directions is also considered , Richards's equation in three dimensions can be derived. Solution of Equation 8 can theoretically provide the spatial and temporal variability of moisture in the soil. However, due to high degree of non linearity of the equation no analytical solution exists for Richards's equation and numerical techniques are used to solve it. For a numerical solution of Richards's equation two essential properties that need to be defined a-priori are (a) relationship between soil water content and hydraulic head, also known as, soil moisture retention curves, and (b) a model that relate hydraulic head to root water uptake. Details about the soil moisture retention curves and numerical techniques used to solve Richards's equation can be found in Simunek et al. (2005). While much literature and field data exist describing the soil moisture retention curves, relatively less information exists about root water uptake models. The root water uptake models generally used, especially, on a watershed scale, are mostly empirical and lack any field verification.

The most common approach used to model root water uptake is to define a sink term S as a function of hydraulic head using the following equation

$$S(h)=\alpha(h)S_p \tag{9}$$

where S(h)[$L^3L^{-3}T^{-1}$] is the actual root water uptake (RWU) from roots subjected to hydraulic or capillary pressure head 'h'. On the right hand side of the equation S_p [$L^3L^{-3}T^{-1}$] is the maximum (also known as potential) uptake of water by the roots. The *a(h)* is a root water uptake stress response function, with its values varying between 0 and 1.

The idea behind conceptualization of **Equation 9** is based on three basic assumptions. The first assumption being , as the soil becomes dryer the amount of water that can be extracted will decrease proportionally. Secondly, the amount of water extracted by the roots is affected by the ambient climatic conditions. Drier and hotter conditions result in more water loss from surface of leaves, hence, initiating more water extraction from the soil. The third and final assumption is that the uptake of water from a particular section of a root is directly proportional to the amount of roots present in that section.

The root water stress response function (α) is a result of the first assumption. Two models commonly used to define α are the Feddes model (Feddes et al. 1978) and the van Genuchten model (van Genuchten 1987). **Figure 7** (a and b, respectively) show the variation of α with decreasing hydraulic head which is same as decreasing water content or increasing soil dryness. Both models for α are empirical and do not involve any plant physiology to define the thresholds for the water stress response function. An interesting

contrast, due to empiricism that is clearly evident is the value of α during saturated conditions. While the Feddes model predict the value of *a* to decrease to zero van Genuchten model predicts totally opposite with α rising to become unity under saturated conditions.

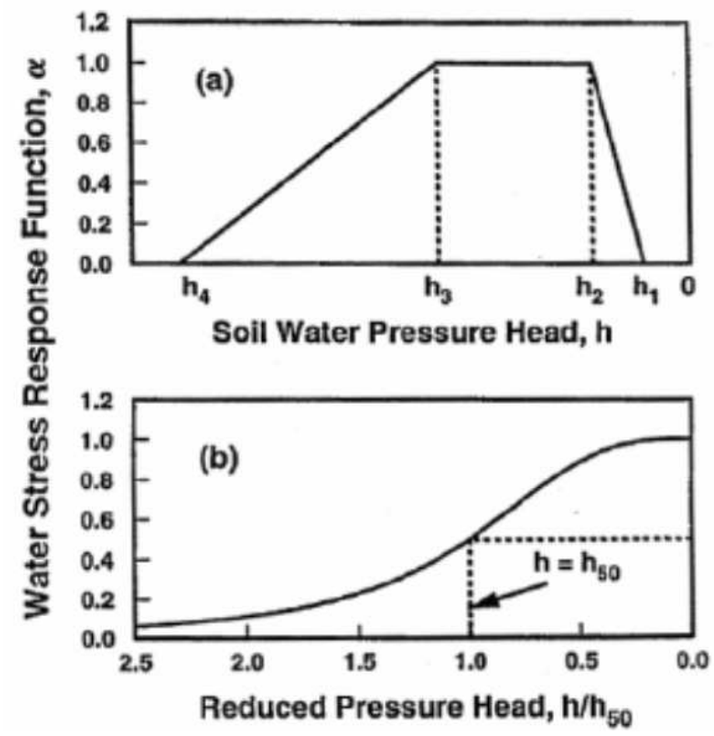

Fig. 7. Water stress response function as given conceptualized by (a) Feddes et al. 1978 and (b) van Genuchten (1980) [Adapted from Simunek et al. 2005].

Recently couple of different models (Li et al. 2001, Li et al. 2006) have been presented to overcome the empiricism in α. However these models are more a result of observation fitting and fail to bring in the plant physiology, which is what causes the changes in the water uptake rate due variation in soil moisture conditions.

Combining the second and the third assumptions in **Equation 9** results in the definition of S_p. S_p for any section of roots is defined as the product of root fraction in that section and the maximum possible water loss by the plant which is also known as the potential evapotranspiration. Potential evapotranspiration is a function of ambient atmospheric conditions and standard models like Penman-Monteith (Allen et al. 1998) are used to calculate the potential evapotranspiration rate. The problem with this definition of Sp is that for any given value of potential evapotranspiration, limiting the value of root water uptake by the root-fraction restrict the amount of water that can be extracted from a particular section. In other words, the amount of water extracted by a particular section of root is directly proportional to the amount of roots present and ignores the amount of ambient soil moisture present. This as will discussed later using field data is a significant limitation especially during dry period when the top soil with maximum roots get dry while the deep soil layer with lesser root mass still have soil moisture available for extraction.

5.2 Use of soil moisture data to estimate root water uptake

For the current analysis, the soil moisture data as described in Section 2 are used. Soil moisture and water-table data from well locations PS-43 and PS-40 were used to determine root water uptake from forested versus grassed land cover. The well PS-43 is referred to as Site A while PS-40 will be called Site B. Hourly averaged data at four hour time step were used for the analysis.

Extensive soil investigations including in-situ and laboratory analysis were performed for the study site. The soil in the study area is primarily sandy marine sediments with high permeability in the surface and subsurface layers. Detailed information about soil and site characteristics can be found in Said et al. (2005), and Trout and Ross (2004). Data for period of record January 2003 to December 2003 were used in this analysis.

van Genuchten (1980) proposed a model relating the water content and hydraulic conductivity with the suction head (soil suction pressure) represented by the following equations

$$S_e = \frac{\theta - \theta_r}{\theta_s - \theta_r} \tag{10}$$

$$\mathrm{h}(\theta) = \frac{(\mathrm{S_e^{\frac{1}{m}}} - 1)^{\frac{1}{\mathrm{n}}}}{\phi} \tag{11}$$

$$K(h) = \begin{cases} K_S S_e^l [1 - (1 - S_e^{1/m})^m & h < 0 \\ K_S & h \geq 0 \end{cases} \tag{12}$$

where m = 1 – 1/n for n > 1, S_e [-] is the normalized water content, varying between 0 and 1. θ is the observed water content, while θ_r and θ_s are the residual and saturated water content values respectively K_S [LT^{-1}] is the hydraulic conductivity when the soil matrix is saturated, l[-] is the pore connectivity parameter assumed to be 0.5 as an average for most soils (Mualem, 1976), and ϕ[L^{-1}], n[-] and m[-] are the van Genuchten empirical parameters. Negative values of hydraulic head (suction head) indicate the water content in the soil matrix is less than saturated while the positive value indicate saturated conditions. From the **Equations 11** and **12**, it is clear that for each type of soil five parameters, namely, K_S, n,ϕ, θ_r and θ_s have to be determined to uniquely define relationship of hydraulic conductivity and water content with soil suction head.

Figure 8 shows the schematics of the vertical soil column which is monitored using eight soil moisture sensors and a pressure transducer measuring the water table elevation, at each of the two locations. Shown also in **Figure 8** is the zone of influence of each sensor along with the elevation of water table and arrows showing possible flow directions. For the purpose of defining moisture retention and hydraulic conductivity curves, each section is treated as a different soil layer and independently parameterized. Hence, for each of the two locations for this particular study eight soil cores from depths corresponding to the zone of influence of each sensor were taken and analyzed (see Shah, 2007 for more details). **Table 2(a)** and **(b)** shows the parameters values that were obtained following the all the soil tests.

Sensor Location Below Land Surface (cm)	θ_S(%)	θ_R(%)	Φ (cm^{-1})	n(-)	K_S(cm/hr)
10	35	3	0.03	1.85	4.212
20	35	3	0.07	1.70	2.520
30	32	3	0.07	1.70	2.520
50	34	3	0.03	1.60	0.803
70	31	3	0.03	1.60	0.005
90	32	3	0.05	1.90	0.005
110	32	3	0.05	1.80	0.005
150	30	3	0.05	1.80	0.001

(a)

Sensor Location Below Land Surface (cm)	θ_S(%)	θ_R(%)	Φ (cm^{-1})	n(-)	K_S(cm/hr)
10	38	3	0.02	1.35	0.0100
20	34	3	0.03	1.35	0.0100
30	31	3	0.03	1.35	0.0100
50	31	3	0.07	1.90	0.0100
70	31	3	0.2	2.20	0.0100
90	31	3	0.2	2.20	0.0004
110	33	3	0.2	2.20	0.0004
150	35	3	0.2	2.10	0.0012

(b)

Table 2. Soil parameters for study locations in (a) Grassland and (b) Forested area.

Once the soil parameterization is complete root water uptake from each section can be calculated. For any given soil layer in the vertical soil column (**Figure 8**), above the observed water table, observed water content and **Equation 11** can be used to calculate the hydraulic head. For soil layers below the water table hydraulic head is same as the depth of soil layer

below the water table due to assumption of hydrostatic pressure. Similarly using **Equation 12** hydraulic conductivity can be calculated. Hence, at any instant in time hydraulic head in each of the eight soil layers can be calculated. To determine total head, gravity head, which is the height of the soil layer above a common datum, has to be added to the hydraulic head.

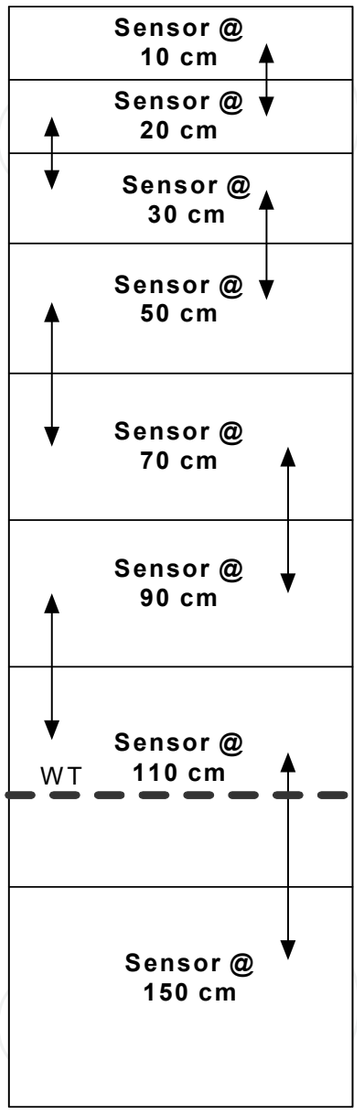

Fig. 8. Schematics of the vertical soil column with location of the soil moisture sensors and water table.

To quantify flow across each soil layer, Darcy's Law (**Equation 7**) is used. Average head values between two consecutive time steps are used to determine the head difference. Also, flow across different soil layers is assumed to be occurring between the midpoints of one layer to another, hence, to determine the head gradient ($\Delta h/l$) the distance between the midpoints of each soil layer is used. The last component needed to solve Darcy's Law is the value of hydraulic conductivity. For flow occurring between layers of different hydraulic conductivities equivalent hydraulic conductivity is calculated by taking harmonic means of

the hydraulic conductivities of both the layers (Freeze and Cherry 1979). Hence for each time step harmonically averaged hydraulic conductivity values (**Equation 13**) were used to calculate the flow across soil layers.

$$K_{eq} = \frac{2K_1K_2}{K_1 + K_2} \tag{13a}$$

where K_1 [LT^{-1}]and K_2 [LT^{-1}]are the two hydraulic conductivity values for any two adjacent soil layers and K_{eq} [LT^{-1}]is the equivalent hydraulic conductivity for flow occurring between those two layers.

Figure 9 shows a typical flow layer with inflow and outflow marked. Now using **simple mass balance** changes in water content at two consecutive time steps can be attributed to net inflow minus the root water uptake (assuming no other sink is present). Equation 6.9 can hence be used to determine root water uptake from any given soil layer

$$RWU = (\theta^t - \theta^{t+1}) - (q_{out} - q_{in}) \tag{13b}$$

Using the described methodology one can determine the root water uptake from each soil layer at both study locations (site A and site B).Time step for calculation of the root water uptake was set as four hours and the root water uptake values obtained were summed up to get a daily value for each soil layer.

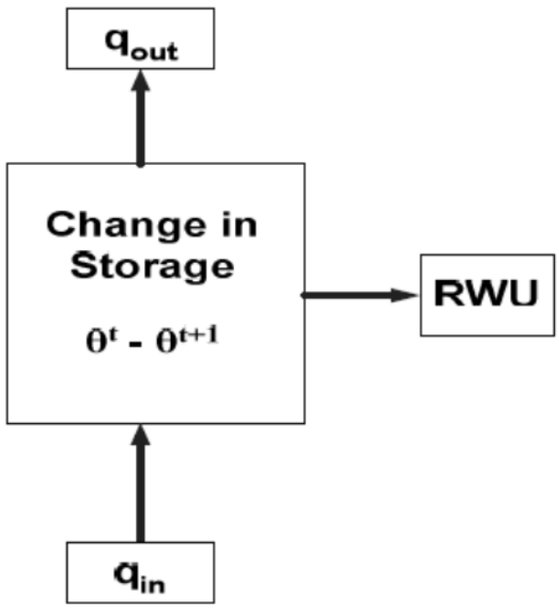

Fig. 9. Schematics of a section of vertical soil column showing fluxes and change in storage.

Using the above methodology root water uptake was calculated from each section of roots for tree and grass land cover from January to December 2003 at a daily time step. **Figure 10** (a and b) shows the variation of root water uptake for a representative period from May 1st to May 15th 2003, This particular period was selected as the conditions were dry and their was no rainfall. Graphs in **Figure 10** (a and b) show the root water uptake variation from

section corresponding to each section. Also plotted on the graphs is the normalized water content, which also gives an indication, of water lost from the section.

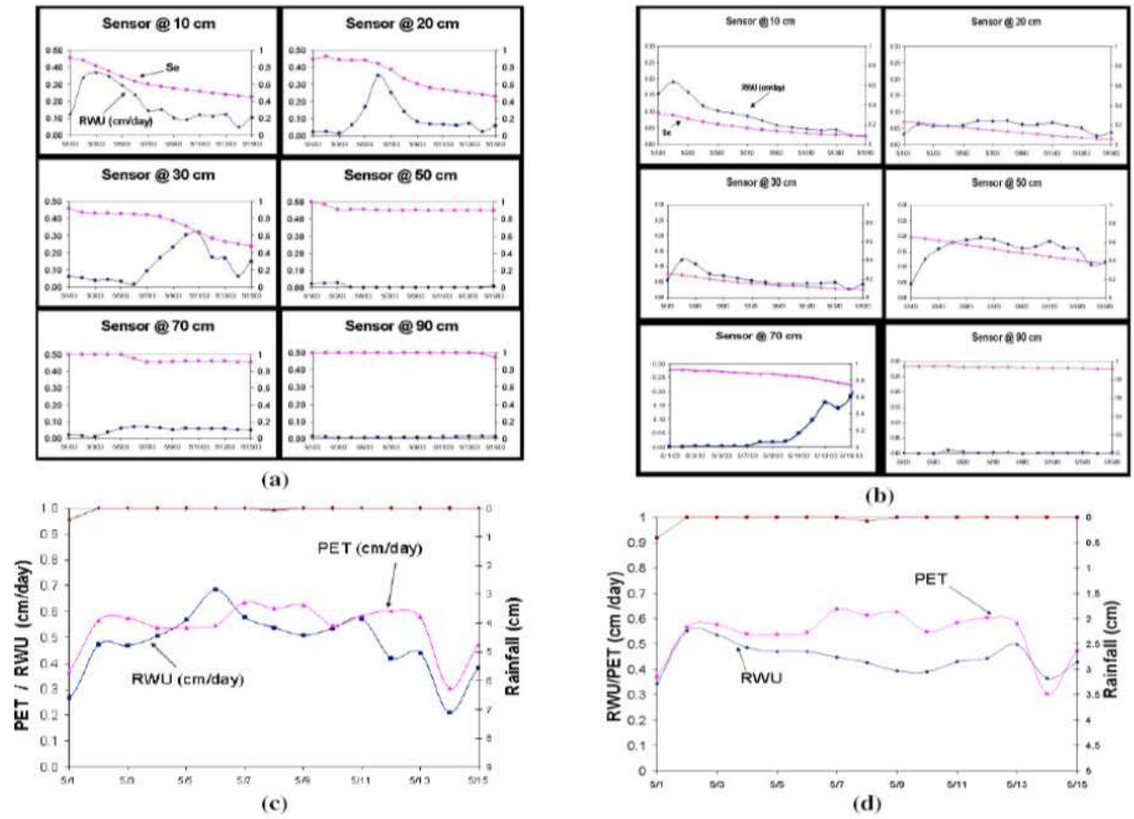

Fig. 10. Root water uptake from sections of soil corresponding to each sensor on the soil moisture instrument for (a, c) Grass land and (b, d) Forest land cover

Figure 10(a) shows the root water uptake from grassed site while panel of graphs in **Figure 10(b)** plots RWU from the forested area. From **Figure 10** (a and b) it can be seen that in both the cases of grass and forest the root water uptake varies with water content and as the top layers starts to get dry, the water uptake from the lower layer increases so as to keep the root water uptake constant clearly indicating that the compensation do take place and hence the models need to account for it. Another important point to note is that in **Figure 10(a)** root water uptake from top three sensors is accounts for the almost all the water uptake while in **Figure 10(b)** the contribution from fourth and fifth sensor is also significant. Also, as will be shown later, in case of forested land cover, root water uptake is observed from the sections that are even deeper than 70 cm below land surface. This is expected owing to the differences in the root system of both land cover types. While grasses have shallow roots, forest trees tend to put their roots deeper into the soil to meet their high water consumptive use.

Figure 10(**c** and **d**) show the values of PET plotted along with the observed values of root water uptake. On comparing the grass versus forested graphs it is evident while the grass is

still evapotranspiring at values close to PET root water uptake from forested land covers is occurring at less than potential. This behavior can be explained by the fact that water content in the grassed region (as shown by the normalized water content graph, Se) is greater than that of the forest and even though the 70 cm sensor shows significant contribution the uptake is still not sufficient to meet the potential demand.

Figure 11 shows an interesting scenario when a rainfall event occurs right after a long dry stretch that caused the upper soil layers to dry out. **Figure 11(a)** shows the root water uptake profile on 5/18/2003 for forested land cover with maximum water being taken from section of soil profile corresponding to 70 cm below the land surface. A rainfall event of 1inch took place on 5/19/2003. As can be clearly seen in **Figure 11(b)** the maximum water uptake shifts right back up to 10 cm below the land surface, clearly showing that the ambient water content directly and quickly affects the root water uptake distribution. **Figure 11(c)** which shows the snapshot on 5/20/2003 a day after the rainfall where the root water uptake starts redistributing and shifting toward deeper wetter layers. In fact this behavior was observed for all the data analyzed for the period of record for both the grass and forested land covers. With roots taking water from deeper wetter layers and as soon as the shallower layer becomes wet the uptakes shifts to the top layers. **Figure 12** (a and b) show a long duration of record spanning 2 months (starting October to end November), with the whiter shade indicating higher root water uptake. From both the figures it is evident that water uptake significantly shifts in lieu of drier soil layers especially in case of forest land cover (**Figure 12(b)**), while in case of grass uptake is primarily concentrated in the top layers.

As a quick summary the results indicate that

a. Assuming RWU as directly proportional to root density may not be a good approximation.
b. Plants adjust to seek out water over the root zone
c. In case of wet conditions preferential RWU from upper soil horizons may take place
d. In case of low ET demands the distribution on ET was found to be occurring as per the root distribution, assuming an exponential root distribution

Hence, traditionally used models are not adequate, to model this behavior. Changes in regard to the modeling techniques as well as conceptualizations, hence, need to occur. Plant physiology is one area that needs to be looked into to see what plant properties affect the water uptake and how can they be modeled mathematically. The next section discusses a modeling framework based on plant root characteristics which can be employed to model the aforesaid observations.

5.3 Incorporation of plant physiology in modeling root water uptake

Any framework to model root water uptake dynamically, will have to explicitly account for all the four points listed above. The dynamic model should be able to adjust the uptake pattern based on root density as well as available water across the root zone. The model should use physically based parameters so as to remove empiricism from the formulation of the equations. For a given distribution of water content along the root zone (observed or modeled) knowledge of root distribution as well as hydraulic characteristics of roots is hence essential to develop a physically based root water uptake model. The following two sections will describe how root distributions can be modeled as well as how do roots need to be characterized to model uptake from root's perspective.

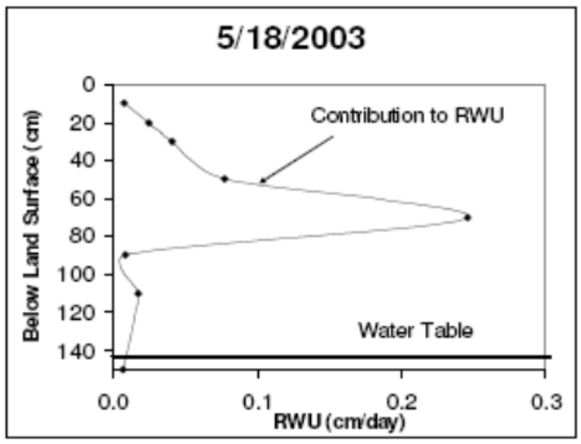

(a)

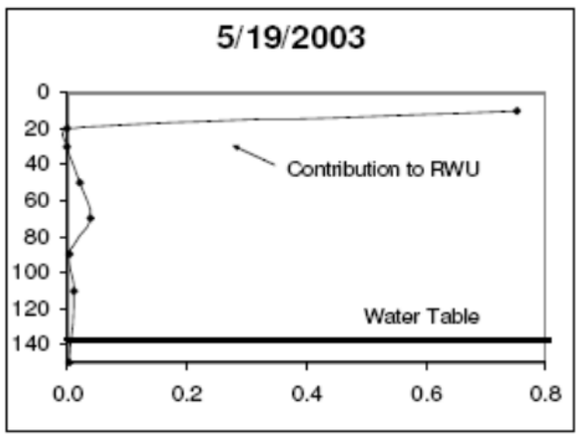

(b)

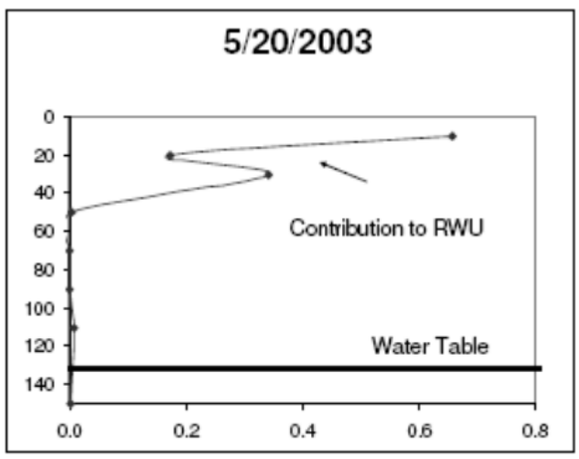

(c)

Fig. 11. Root water uptake variation due to a one inch rainfall even on 5/19/2003.

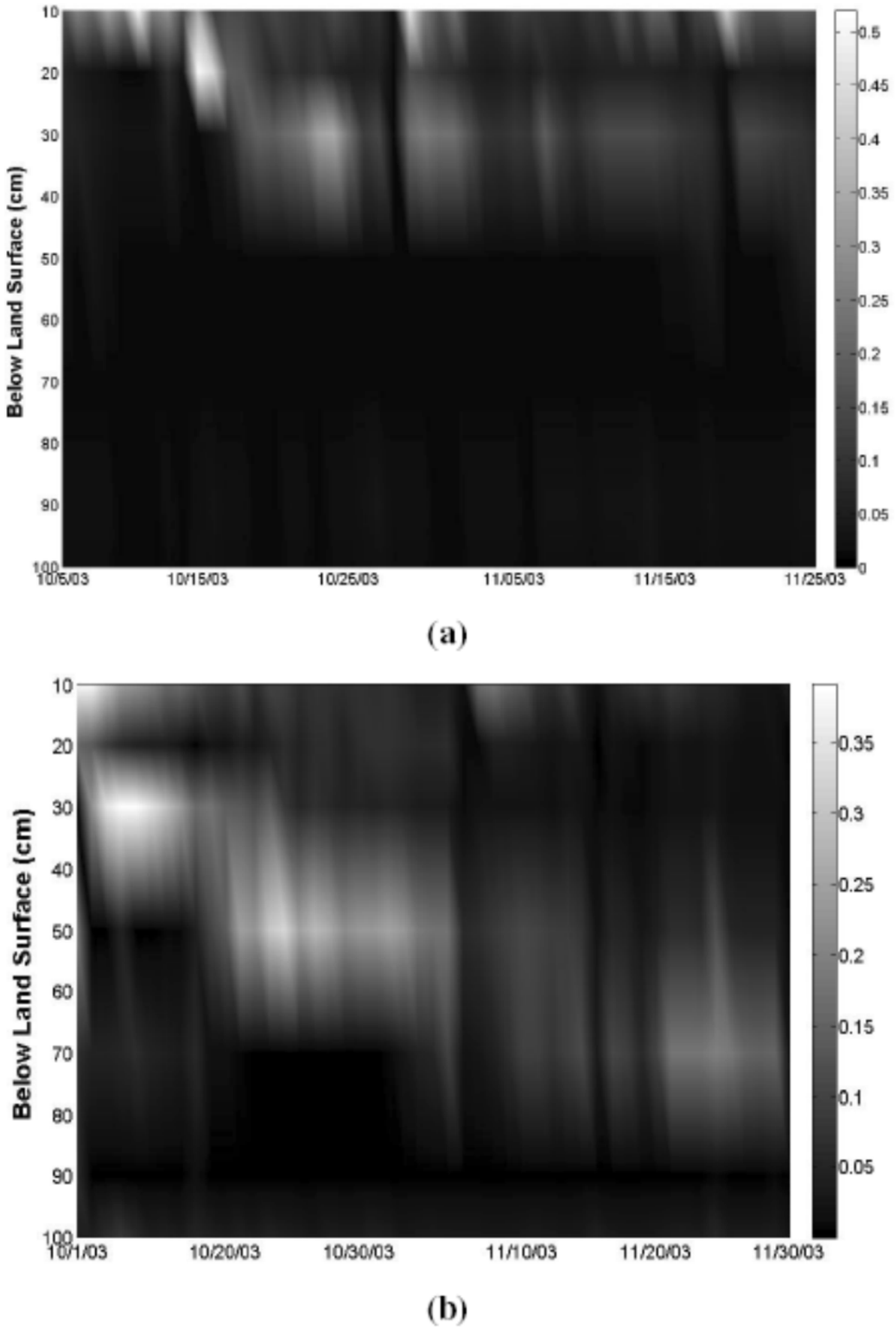

Fig. 12. Daily root water uptake variation for two October and November 2003 for (a) grass land cover and (b) forested land cover.

5.3.1 Root distribution

Schenk and Jackson (2002) expanded an earlier work of Jackson et al. (1996) to develop a global root database having 475 observed root profiles from different geographic regions of the world. It was found that by varying parameter values the root distribution model given by Gale and Grigal (1987) can be used with sufficient accuracy to describe the observed root distributions. **Equation 14** describes the root distribution model.

$$Y = 1 - \gamma^{d} \tag{14}$$

where Y is the cumulative fraction of roots from the surface to depth d, and γ is a numerical index of rooting distribution which depends on vegetation type. **Figure 13** shows the observed distribution (shown by data points) versus the fitted distribution using **Equation 14** for different vegetation types. The figure clearly indicates the goodness of fit of the above model. Hence, for a given type of vegetation a suitable γ can be used to describe the root distribution.

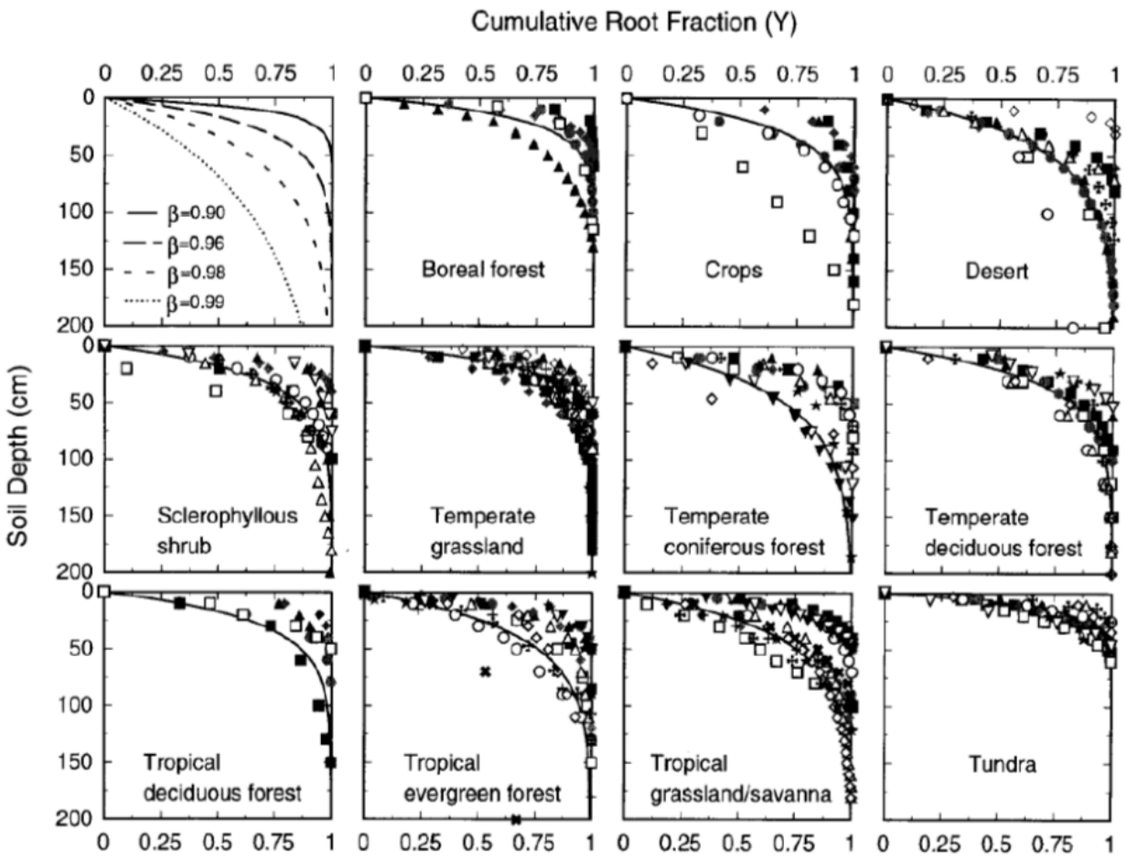

Fig. 13. Observed and Fitted Root Distribution for different type of land covers. [Adapted from Jackson et al. 1996]

5.3.2 Hydraulic characterization of roots

Hydraulically, soil and xylem are similar as they both show a decrease in hydraulic conductivity with reduction in soil moisture (increase in soil suction). For xylem the

relationship between hydraulic conductivity and soil suction pressure is called 'vulnerability curve' (Sperry et al. 2003) (see **Figure 14**). The curves are drawn as a percentage loss in conductivity rather than absolute value of conductivity due to the ease of determination of former. Tyree et al (1994) and Hacke et al (2000) have described methods for determination of vulnerability curves for different types of vegetation.

Commonly, the stems and/or root segments are spun to generate negative xylem pressure (as a result of centrifugal force) which results in loss of hydraulic conductivity due to air seeding into the xylem vessels (Pammenter and Willigen 1998). This loss of hydraulic conductivity is plotted against the xylem pressure to get the desired vulnerability curve.

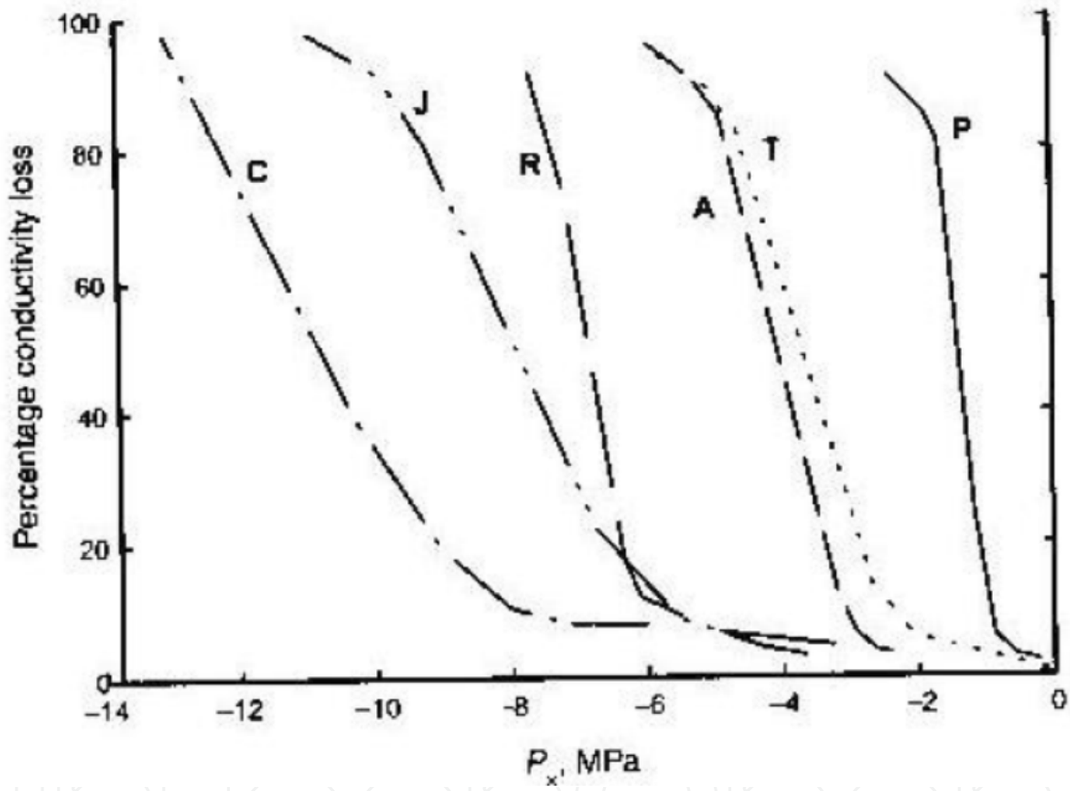

Fig. 14. Vulnerability curves for various species. [Adapted from Tyree, 1999]

For different plant species the vulnerability curve follows an S-Shape function, see **Figure 14** (Tyree 1999). In **Figure 14**, y-axis is percentage loss of hydraulic conductivity induced by the xylem pressure potential Px, shown on the x-axis. C= Ceanothus megacarpus, J = Juniperus virginiana, R = Rhizphora mangel, A = Acer saccharum, T= Thuja occidentalis, P = Populus deltoids.

Pammenter and Willigen (1998) derived an equation to model the vulnerability curve by parametrizing the equation for different plant species. **Equation 15** describes the model mathematically.

$$PLC = \frac{100}{1 + e^{a.(P - P_{50\,PLC})}} \tag{15}$$

where PLC denotes the percentage loss of conductivity P_{50PLC} denotes the negative pressure causing 50% loss in the hydraulic conductivity of xylems, P represents the negative pressure and a is a plant based parameter. **Figure 15** shows the model plotted against the data points for different plants. Oliveras et al. (2003) and references cited therein have parameterize the model for different type of pine and oak trees and found the model to be successful in modeling the vulnerability characteristics of xylem.

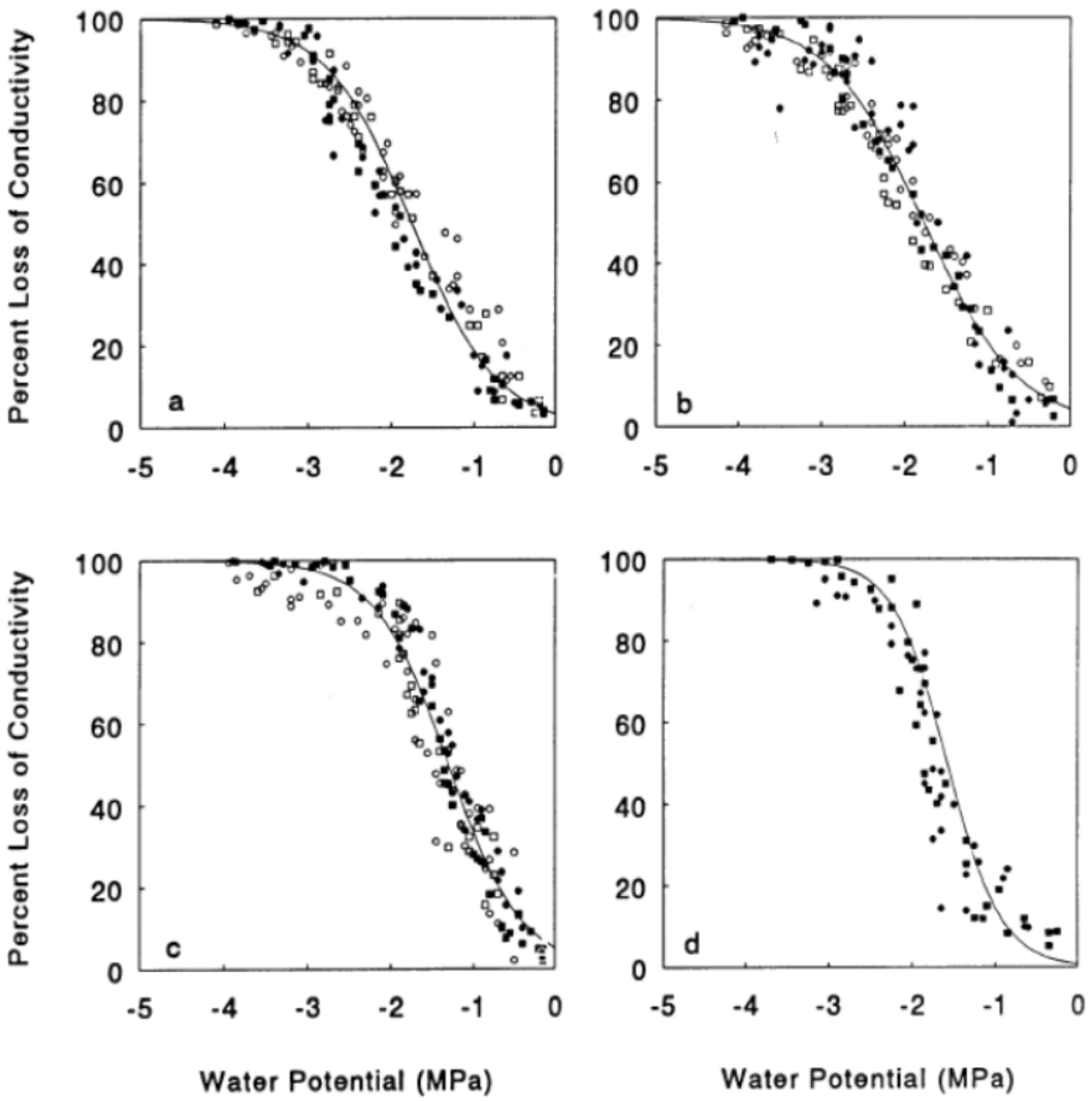

Fig. 15. Observed values and fitted vulnerability curve for roots and stem sections of different Eucylaptus trees. [Adapted from Pammenter and Willigen, 1998].

The knowledge of hydraulic conductivity loss can be used analogous to the water stress response function *a* (**Equation 9**) by scaling PLC from 0 to 1 and converting the suction pressure to water head. The advantage of using vulnerability curves instead of Feddes or van Genuchten model is that vulnerability curves are based on xylem hydraulics and hence can be physically characterized for each plant species.

5.3.3 Development of a physically based root water uptake model

The current model development is based on model conceptualization proposed by Jarvis (1989) however the parameters for the current model are physically defined and include plant physiological characteristics.

For a given land cover type **Equation 14** and **15** can be parameterize to determine the root fraction for any given segment in root zone and percentage loss of conductivity for a given soil suction pressure. For consistency of representation percentage loss of conductivity will be hence forth represented by α (scaled between 0 and 1 similar to **Equation 9**) and will be called stress index.

For any section of root zone, for example i^{th} section, root fraction can be written as R_i and stress index, determined from vulnerability curve and ambient soil moisture condition, can be written as a_i. Average stress level $\bar{\alpha}$ over the root zone can be defined as the

$$\bar{\alpha} = \sum_{i=1}^{n} R_i \alpha_i \tag{16}$$

where n represents the number of soil layers and the other symbols are as previously defined. Thus, as can be seen from **Equation 16** the average stress level $\bar{\alpha}$ combines the effect of both the root distribution and the available water content (via vulnerability curve).

As shown in **Figure 12(b)** if there is available moisture in the root zone, plant can transpire at potential by increasing the uptake from the lower wetter section of the roots. In terms of modeling it can be conceptualized that above a certain critical average stress level ($\bar{\alpha}_C$) plants can transpire at potential and below $\bar{\alpha}_C$ the value of total evapotranspiration decreases. The decrease in the ET value can be modeled linearly as shown by Li et al (2001). The graph of average stress level versus ET (expresses as a ratio with potential ET rate) can hence be plotted as shown in **Figure 16**. In **Figure 16**, ET_a is the actual ET out of the soil column while ET_p is the potential value of ET. **Figure 16** can be used to determine the value of actual ET for any given average stress level.

Once the actual ET value is known, the contribution from individual sections can be modeled depending on the weighted stress index using the relationship defined by

$$S_i = \left(\frac{E_a}{\Delta Z_i}\right)\left(\frac{R_i \alpha_i}{\bar{\alpha}}\right) \tag{17}$$

where S_i defined as the water uptake from the i^{th} *section*, ΔZi is the depth of i^{th} section and other symbols are as previously defined

Jarvis (1989) used empirical values to simulate the behavior of the above function and **Figure 17** shows the result of root water uptake obtained from his simulation. The values next to each curve in **Figure 17** represent the day after the start of simulation and actual ET rate as expressed in mm/day. On comparison with **Figure 12**, the model successfully reproduced the shift in root water uptake pattern with the uptake being close to potential value (ET_P = 5.0 mm/d) for about a month from the start of simulation. The decline in ET rate occurred long after the start of the simulation in accordance with the observed values. The model was successful not only in simulating peak but also in the observed magnitude of the root water uptake.

From the above analysis it can be concluded that the root water uptake is just not directly proportional to the distribution of the roots but also depends on the ambient water content. Under dry conditions roots can easily take water from deeper wetter soil layers.

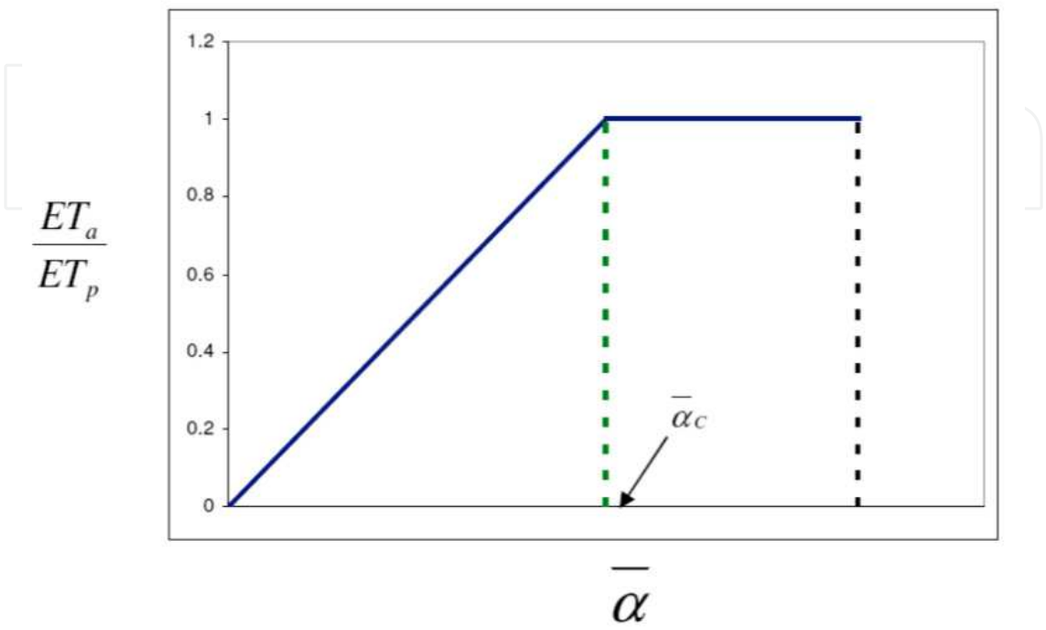

Fig. 16. Variation of ratio of actual to potential ET with location of the critical stress level.

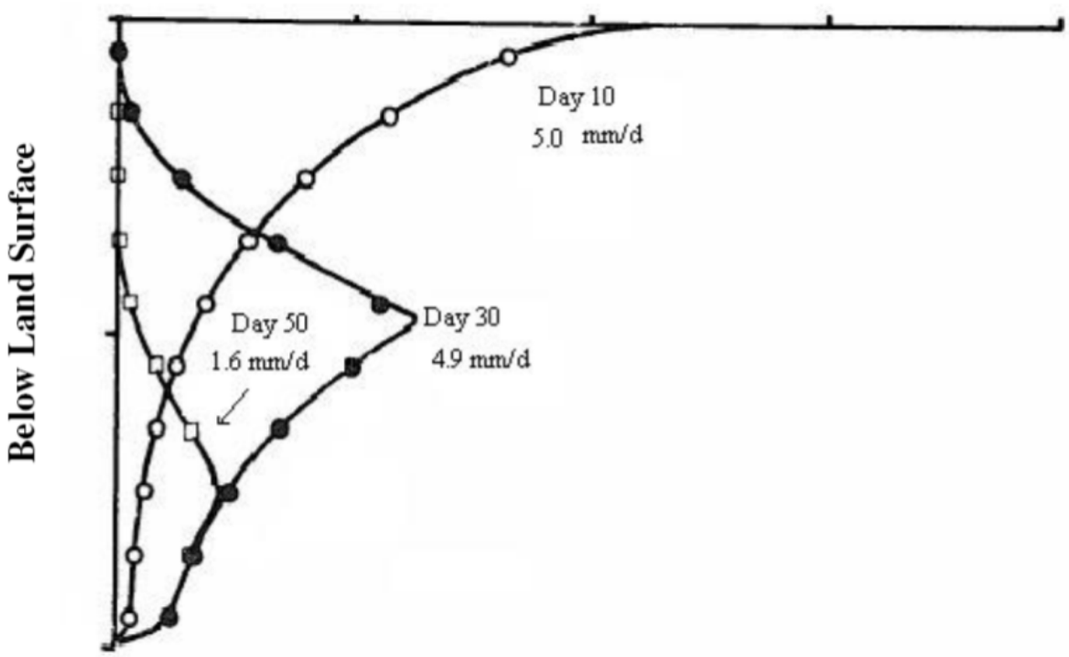

Fig. 17. Variation in the vertical distribution of root water uptake, at different times. [Adapted from Jarvis (1989)]

The methodology described here involves initial laboratory analyses to determine the hydraulic characteristics of the plant. However, once a particular plant specie is characterized then the parameters can be use for that specie elsewhere under similar conditions. The approach shows that eco-hydrological framework has great potential for improving predictive hydrological modeling.

6. Conclusion

The chapter described a method of data collection for soil moisture and water table that can be used for estimation of evapotranspiration. Also described in the chapter is the use of vertical soil moisture measurements to compute the root water uptake in the vadose zone and use that uptake to validate a root water uptake model based on plant physiology based root water uptake model. As evaporation takes place primarily from the first few centimeters (under normal conditions) of the soil profile and the biggest component of the ET is the root water uptake. Hence to improve our estimates of ET, which constitutes ~70% of the rainfall, the estimation and modeling of root water uptake needs to be improved. Eco-hydrology provides one such avenue where plant physiology can be incorporated to better represent the water loss. Also, hydrological model incorporating plant physiology can be modified easily in future to be used to predict land-cover changes due to changes in rainfall pattern or other climatic variables.

7. References

Allen RG, Pereira LS, Raes D, Smith M.1998. Crop evapotranspiration—guidelines for computing crop water requirements.FAO Irrigation & Drainage Paper 56. FAO, Rome

Bidlake, W. R., W.M.Woodham, and M.A.Lopez. 1993. Evapotranspiration from areas of native vegetation in Wets-Central Florida: U.S. Geological Survey open file report 93-415, 35p.

Brutsaert, W.1982. Evaporation into the Atmosphere: Theory, History, and Applications. Kluwer Academic Publishers, Boston, MA.

Doorenbos, J., and W.O.Pruitt. 1977. Crop Water Requirements. FAO Irrigation and drainage paper 24. Food and agricultural organization of the United Nations, Rome.

Fares, A. and A.K. Alva. 2000. Evaluating the capacitance probes for optimal irrigation of citrus through soil moisture monitoring in an Entisol profile. Irrigation. Science 19:57–64.

Fayer,M.J. and D.Hillel.1986. Air Encapsulation I - Measurement in a field soil. Soil Science Society of America Journal. 50:568-572.

Feddes,R.A., P.J.Kowalik, and H.Zaradny. 1978. Simulation of field water use and crop yield. New York: John Wiley & Sons.

Freeze,R. and J.Cherry. 1979. Groundwater. Prentice Hall, Old Tappan, NJ.

Hacke.U.G., J.S.Sperry, and J.Pittermann. 2000. Drought Experience and Cavitation Resistance in Six Shrubs from the Great Basin, Utah. Basic Applied Ecology 1:31-41.

Hillel,D. 1998. Environmental soil physics. Academic Press, New York, NY

Jackson, R.B., J.Canadell, J.R.Ehleringer, H.A.Mooney, O.E.Sala, and E.D.Schulze. 1996. A global analysis of root distributions for terrestrial biomes. Oecologia 108:389-411.

Jarvis.N.J. 1989. A Simple Empirical Model of Root Water Uptake. Journal of Hydrology.107:57-72.

Kite, G.W., and P. Droogers. 2000. Comparing evapotranspiration estimates from satellites, hydrological models and field data. Journal of Hydrology 229:3–18.

Knowles, L., Jr. 1996. Estimation of evapotranspiration in the Rainbow Springs and Silver Springs basin in north-central Florida. Water resources investigation report. 96-4024. USGS, Reston, VA.

Li, K.Y., R.De jong, and J.B. Boisvert. 2001. An exponential root-water-uptake model with water stress compensation. Journal of hydrology 252:189-204.

Li,K.Y., R.De Jong, and M.T.Coe. 2006. Root water uptake based upon a new water stress reduction and an asymptotic root distribution function. Earth Interactions 10 (paper 14):1-22.

Mahmood, R. and K.G. Hubbard. 2003. Simulating sensitivity of soil moisture and evapotranspiration under heterogeneous soils and land uses. Journal of Hydrology. 280:72–90.

Meyboom, P. 1967. Ground water studies in the Assiniboine river drainage basin: II. Hydrologic characteristics of phreatophytic vegetation in south-central Saskatchewan. Geological Survey of Canada Bulletin 139, no.64.

Monteith, J. L. 1965. Evaporation and environment. *In* G.E.Fogg (ed). The state and movement of water in living organisms. Symposium of the Society of Experimental Biology: San Diego, California, Academic Press, New York, p.205-234

Morgan,K.T., L.R.Parsona, T.A. Wheaton, D.J.Pitts and T.A.Oberza. 1999. Field calibration of a capacitance water content probe in fine sand soils. Soil Science Society of America Journal 63: 987-989.

Mo, X., S. Liu, Z. Lin, and W. Zhao. 2004. Simulating temporal and spatial variation of evapotranspiration over the Lushi basin. Journal of Hydrology 285:125–142.

Mualem, Y. 1976. A new model predicting the hydraulic conductivity of unsaturated porous media. Water Resources Research 12(3):513-522.

Nachabe, M., N.Shah, M.Ross, and J.Vomacka. 2005. Evapotranspiration of two vegetation covers in a shallow water table environment. Soil Science Society of America Journal 69:492-499.

Oliveras,I., J.Martinez-Vilalta, T.Jimenez-Ortiz, M.J Lledo, A.Escarre, and J.Pinol. 2003. Hydraulic Properties of Pinus Halepensis, Pinus Pinea, and Tetraclinis Articulata in a Dune Ecosystem of Eastern Spain. Plant Ecology 169:131-141.

Pammenter.N.W. and C.V.Willigen. 1998. A Mathematical and Statistical Analysis of the Curves Illustrating Vulnerability of Xylem to Cavitation. Tree Physiology 18:589-593.

Priestley, C.H.B., and Taylor, R.J. 1972. On the assessment of surface heat flux and evaporation using large-scale parameters. Monthly Weather Review 100(2): 81-92.

Richards.L.A .1931. Capillary conduction of liquids through porous mediums, Journal of Applied Physics, 1(5), 318-333.

Said , A., M.Nachabe, M.Ross, and J.Vomacka. 2005. Methodology for estimating specific yield in shallow water environment using continuous soil moisture data. ASCE Journal of Irrigation and Drainage Engineering 131, no.6:533-538.

Schenk, H.J. and R. B. Jackson. 2002. Rooting Depths, Lateral Root Spreads and Below-Ground/Above-Ground Allometries of Plants in Water-Limited Ecosystems. The Journal of Ecology 90(3):480-494.

Shah,N. 2007. Vadose Zone Processes Affecting Water Table Fluctuations – Conceptualization and Modeling Considerations. PhD Disseration, University of South Florida, Tampa, Fl, 233 pp.

Shah, N., M. Ross, and A. Said. 2007. Vadose Zone Evapotranspiration Distribution Using One-Dimensional Analysis and Conceptualization for Integrated Modeling. Proceedings of ASCE EWRI conference, May 14th –May 19th 2007, Tampa.

Simunek, J., M. Th. van Genuchten and M. Sejna. 2005. The HYDRUS-1D software package for simulating the movement of water, heat, and multiple solutes in variably saturated media, version 3.0, HYDRUS software series 1. Department of Environmental Sciences, University of California Riverside, Riverside, California, USA, 270 pp.

Sperry, J.S., V.Stiller, and U.G.Hacke. 2003 Xylem Hydraulics and the Soil-Plant-Atmosphere Continuum: Oppurtunities and Unresolved Issues. Agronomy Journal 95:1362-1370.

Sumner, D.M. 2001. Evapotranspiration from a cypress and pine forest subjected to natural fires, Volusia County, Florida, 1998-99. Water Resources Investigations Report 01-4245. USGS, Reston, VA.

Sumner, D. 2006.Adequacy of selected evapotranspiration approximations for hydrological simulation. Journal of the American Water Resources Association. 42(3):699- 711.

Thornthwaite, C.W. 1948. An approach toward a rational classification of climate. Geographic Review 38:55-94.

Trout, K., and M.Ross. 2004. Intensive hydrologic data collection in as small watershed in West-Central Florida. Hydrological Science and Technology 21(1-4):187-197.

Tyree, M.T. S.Yang, P.Cruiziat, and, B.Sinclair. 1994. Novel Methods of Measuring Hydraulic Conductivity of Tree Root Systems and Interpretation Using AMAIZED. Plant Physilogy 104:189-199

van Genuchten, M.Th. 1980. A closed-form equation for predicting the hydraulic conductivity of unsaturated soils. Soil Science Society of America Journal 44:892-898.

van Genuchten, M. Th.1987. A numerical model for water and solute movement in and below the root zone. Research report No 121, U.S. Salinity laboratory, USDA, ARS, Riverside, California, 221pp.

Yang, J., B. Li, and S. Liu. 2000. A large weighing lysimeter for evapotranspiration and soil water-groundwater exchange studies. Hydrological Processes 14:1887–1897.

White,W.N. 1932.A method of estimating ground-water supplies based on discharge by plants and evaporation from soil: Results of investigation in Escalante Valley, Utah. Water-Supply Paper 659-A.

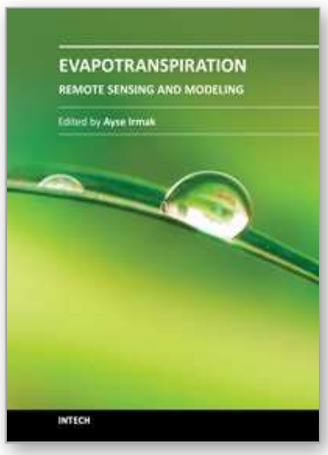

Evapotranspiration - Remote Sensing and Modeling

Edited by Dr. Ayse Irmak

ISBN 978-953-307-808-3
Hard cover, 514 pages
Publisher InTech
Published online 18, January, 2012
Published in print edition January, 2012

This edition of Evapotranspiration - Remote Sensing and Modeling contains 23 chapters related to the modeling and simulation of evapotranspiration (ET) and remote sensing-based energy balance determination of ET. These areas are at the forefront of technologies that quantify the highly spatial ET from the Earth's surface. The topics describe mechanics of ET simulation from partially vegetated surfaces and stomatal conductance behavior of natural and agricultural ecosystems. Estimation methods that use weather based methods, soil water balance, the Complementary Relationship, the Hargreaves and other temperature-radiation based methods, and Fuzzy-Probabilistic calculations are described. A critical review describes methods used in hydrological models. Applications describe ET patterns in alpine catchments, under water shortage, for irrigated systems, under climate change, and for grasslands and pastures. Remote sensing based approaches include Landsat and MODIS satellite-based energy balance, and the common process models SEBAL, METRIC and S-SEBS. Recommended guidelines for applying operational satellite-based energy balance models and for overcoming common challenges are made.

INTECH
open science | open minds

InTech Europe
University Campus STeP Ri
Slavka Krautzeka 83/A
51000 Rijeka, Croatia
Phone: +385 (51) 770 447
Fax: +385 (51) 686 166
www.intechopen.com

InTech China
Unit 405, Office Block, Hotel Equatorial Shanghai
No.65, Yan An Road (West), Shanghai, 200040, China
中国上海市延安西路65号上海国际贵都大饭店办公楼405单元
Phone: +86-21-62489820
Fax: +86-21-62489821

IntechOpen